Insight into Resolution Enhancement in Generalized Two-Dimensional Correlation Spectroscopy

Lu Ma,[a] Vitali Sikirzhytski,[b] Zhenmin Hong,[a] Igor K. Lednev,[b] Sanford A. Asher[a,*]

[a]Department of Chemistry, University of Pittsburgh, Pittsburgh, Pennsylvania 15260, USA
[b]Department of Chemistry, University at Albany, Albany, New York 12222, USA

Generalized two-dimensional correlation spectroscopy (2D-COS) can be used to enhance spectral resolution in order to help differentiate highly overlapped spectral bands. Despite the numerous extensive 2D-COS investigations, the origin of the 2D spectral resolution enhancement mechanism(s) is not completely understood. In the work here, we studied the 2D-COS of simulated spectra in order to develop new insights into the dependence of 2D-COS spectral features on the overlapping band separations, their intensities and bandwidths, and their band intensity change rates. We found that the features in the 2D-COS maps that are derived from overlapping bands were determined by the spectral normalized half-intensities and the total intensity changes of the correlated bands. We identified the conditions required to resolve overlapping bands. In particular, 2D-COS peak resolution requires that the normalized half-intensities of a correlating band have amplitudes between the maxima and minima of the normalized half-intensities of the overlapping bands.

Index Headings: **Two-dimensional correlation spectroscopy; Resolution enhancement; Overlapping bands; Normalized half-intensity.**

INTRODUCTION

Two-dimensional correlation spectroscopy (2D-COS) was first introduced by Isao Noda[1–4] as a mathematical technique to investigate the behavior of a system in response to external perturbations (temperature, pH, concentration, time, etc.). Two-dimensional COS has been successfully applied to analyze nuclear magnetic resonance, infrared, Raman, ultraviolet–visible light, fluorescence spectra, etc.[3–8] This technique establishes correlations between spectral intensity variations within a set of spectra by generating 2D maps, known as 2D synchronous and asynchronous spectra. Information such as the similarity, direction, and sequential order of correlated spectral intensity variations can be extracted by studying the 2D correlation peak features.[4,9] 2D-COS also enhances spectral resolution by spreading highly overlapped band features along a second dimension.[6,10–12] Overlapping peaks are thought to be signaled by the appearance of correlation peaks in 2D synchronous and asynchronous spectra. For these cases, 2D-COS is a powerful tool to investigate complex spectral data from polymers, colloids, proteins, peptides, pharmaceuticals, etc.[8,13,14]

Despite the utility of 2D-COS resolution enhancement, as recognized in 1990s,[3,15] and its wide use, the underlying resolution enhancement mechanism(s) is not well understood.[16–18] Two-dimensional synchronous or asynchronous correlated peaks occur if the intensities of two spectral features

change in phase or out of phase with each other.[4] Although it is generally expected that the number of correlation peaks will be equal to the number of overlapping bands, this does not always occur. For example, Yu et al. found (surprisingly) the presence of three correlation peaks in the 2D-COS spectra, derived from one narrow band embedded within a single broad band.[19]

Previous studies indicated that artifactual, misleading features can be generated in 2D-COS spectra, which are easily misinterpreted to indicate the presence of overlapping bands. For example, bandwidth changes and band shifting can generate peculiar 2D-COS peak features that do not originate from real resolved spectral bands.[18,20–24] It is difficult to distinguish single-band peak shifts from intensity changes from two overlapped bands, since both spectral changes generate similar 2D spectral patterns.[24,25] These results indicate that great care must be paid to correctly interpret any apparent resolution enhancement 2D-COS spectral feature.

Much effort has been expended to understand the origin of 2D-COS spectral features. Most recently, a diagnostic test was developed by Jung et al. to distinguish features resulting from single-band shifts from those resulting from overlapped bands.[26] Czarnecki's simulations show that multiple overlapping bands with changing relative intensities can give features very similar to 2D-COS spectral features, which result from frequency shifts of a single band. Thus, there can be confusion discriminating between peak shifts and those features deriving from overlapping bands.[27]

It is clear that a deeper understanding of the origin of 2D-COS spectral features is necessary in order to interpret 2D-COS resolution enhancement features correctly. Thus, in the work here, we examine the dependence of 2D-COS spectral features on overlapping band separations, band intensities and band-widths, and the rates of band intensity changes. We identify the conditions required to resolve overlapping bands, and discuss the features in the 2D-COS maps that signal overlapping bands.

EXPERIMENTAL

2D Correlation Analysis. Noda proposed a practical method to compute generalized 2D correlation spectra.[4,28] Assuming a set of m spectra collected over perturbation t at equally spaced increments, the 2D synchronous $\Phi(\nu_1, \nu_2)$ and asynchronous $\Psi(\nu_1, \nu_2)$ correlation intensities at ν_1 and ν_2 are calculated:

$$\Phi(\nu_1, \nu_2) = \frac{1}{m-1} \tilde{y}(\nu_1)^T \tilde{y}(\nu_2) \qquad (1)$$

$$\Psi(\nu_1, \nu_2) = \frac{1}{m-1} \tilde{y}(\nu_1)^T N \, \tilde{y}(\nu_2) \qquad (2)$$
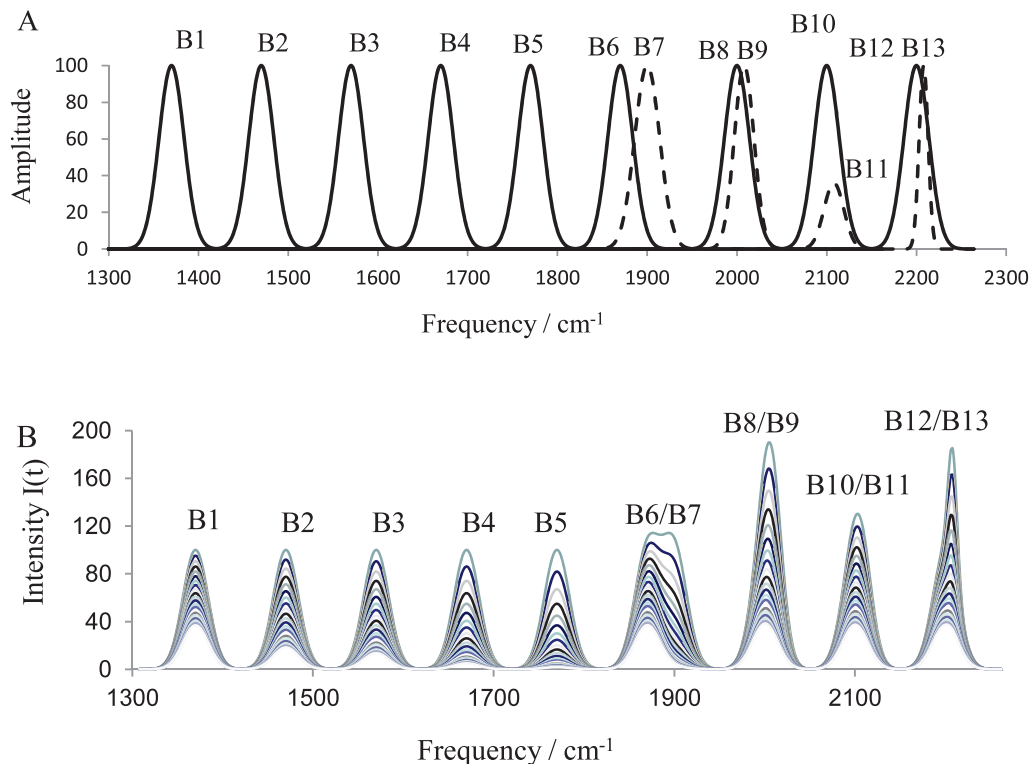
APPLIED SPECTROSCOPY **283**

FIG. 1. (A) Thirteen Gaussian band spectra. (B) Simulated spectra.

where $\tilde{y}(v_i)$ is the dynamic spectral intensity matrix:

$$\tilde{y}(v_i) = \tilde{y}(v_i, t) = \begin{bmatrix} \tilde{y}(v_i, t_1) \\ \tilde{y}(v_i, t_2) \\ \cdots \\ \tilde{y}(v_i, t_m) \end{bmatrix} \qquad (3)$$

$\tilde{y}(v_i, t_j)$ is the dynamic spectral signal at v_i and time t_j defined by the following equation:

$$\tilde{y}(v_i, t_j) = y(v_i, t_j) - \frac{1}{m}\sum_{k=1}^{m} y(v_i, t_k) \qquad (4)$$

where $y(v_i, t_j)$ is the measured spectral signal at v_i and time t_j. N in Eq. (2) is the Hilbert–Noda matrix, given by:

$$N = \frac{1}{\pi} \begin{bmatrix} 0 & 1 & \frac{1}{2} & \frac{1}{3} & \cdots \\ -1 & 0 & 1 & \frac{1}{2} & \cdots \\ -\frac{1}{2} & -1 & 0 & 1 & \cdots \\ -\frac{1}{3} & -\frac{1}{2} & -1 & 0 & \cdots \\ \cdots & \cdots & \cdots & \cdots & \cdots \end{bmatrix} \qquad (5)$$

The synchronous spectrum is the inner product of two dynamic spectral vectors measured at two different spectral frequencies, v_1 and v_2. The asynchronous spectrum is the inner product of the dynamic spectral vectors and the orthogonal Hilbert–Noda matrix.

The 2D correlation spectra here were calculated as discussed above. We consider here only those cross-peaks located below the correlation diagonal and label them as (v_1, v_2), where v_1, v_2 refer to the abscissa and ordinate spectral frequencies.

Simulations. The simulated spectra used here were composed of 13 Gaussian bands, $I_{i,0}(v) = A_i e^{-\frac{(v-v_{ci})^2}{2w_i^2}}$, as shown in Fig. 1A, where w_i determines the full bandwidth at half height [FWHH = $2(2\ln2)^{1/2}w_i$], v_{ci} is the band center frequency, v is the spectral frequency, and A_i is the maximum amplitude of the ith Gaussian band. The ith band intensity decreases exponentially with time as $f_i(t) = e^{-k_i t}$. In the following discussion, Bi refers to the ith band.

The Gaussian band parameters and their intensity change functions are summarized in Table I. The first five bands have identical maximum intensities and bandwidths and are separated by 100 cm^{-1}. The other eight bands are paired to form four overlapping bands: B6/B7; B8/B9; B10/B11; and B12/B13, B6, and B7 are separated by 30 cm^{-1}, while B8 and B9, B10 and B11, and B12 and B13 are separated by 8 cm^{-1}. All bands have $w = 14$ cm^{-1}, except for B9 and B11, where $w = 11$ cm^{-1}, and B13 with $w = 5$ cm^{-1}. All bands have $A = 100$, except for B11 where $A = 36$.

The B1/B5 band intensity change rate constants k are 0.05, 0.085, 0.1, 0.15, and 0.2 s^{-1}, respectively. For B6, B8, B10, and B12, $k = 0.05$ s^{-1}, and for B7, B9, B11, and B13 $k = 0.2$ s^{-1}.

Figure 1B shows the simulated spectra:

$$I(v, t) = \sum_{i=1}^{m} f_i(t) I_{i,0}(v) \qquad (6)$$

TABLE I. Gaussian band parameters and the band intensity change functions.

Band	$f(t)$	v_c (cm^{-1})	A	w (cm^{-1})
B1	$e^{-0.05t}$	1370	100	14
B2	$e^{-0.085t}$	1470	100	14
B3	$e^{-0.1t}$	1570	100	14
B4	$e^{-0.15t}$	1670	100	14
B5	$e^{-0.2t}$	1770	100	14
B6	$e^{-0.05t}$	1870	100	14
B7	$e^{-0.2t}$	1900	100	14
B8	$e^{-0.05t}$	2000	100	14
B9	$e^{-0.2t}$	2008	100	11
B10	$e^{-0.05t}$	2100	100	14
B11	$e^{-0.2t}$	2108	36	11
B12	$e^{-0.05t}$	2200	100	14
B13	$e^{-0.2t}$	2208	100	5

where $m = 13$ is the number of the Gaussian bands, and $f_i(t)$ is defined as the intensity change coefficient, calculated as $f_i(t) = e^{-k_i t}$.

The simulation consists of 21 spectra, with spectrum 1 the starting spectrum at $t = 0$ s. The time interval between spectra is 1 s. The spacing between spectral data points is 2 cm^{-1}.

Spectral Normalization. The normalized spectral intensity $F(v, t)$ is calculated as:

$$F(v,t) = \frac{I(v,t) - I(v,0)}{I(v,T) - I(v,0)} \quad (7)$$

where $I(v, t)$ is the spectral intensity at t.[29] Normalization makes the spectral intensities range from 0 to 1 over the total perturbation time T. The results of spectral signal intensity normalization are shown in Fig. 2. Eq. (7) can be rewritten as:

$$I(v,t) = K(v)F(v,t) + b(v) \quad (8)$$

where $K(v) = I(v, T) - I(v, 0)$, and $b(v) = I(v, 0)$. The normalized half-intensity (NHI) is defined as the normalized intensity at $t = T/2$, as shown in Fig. 2B. Note that the 2D-COS spectra in this paper were calculated from the original spectra, without normalization. The NHI parameter is used to explain the 2D-COS spectral features.

Recently, as a further interpretation of Noda's sequential rule,[4] Yu et al. proposed the following correlation of the signs of the synchronous and asynchronous cross-peaks to the relative values of the NHI at v_1 and v_2 (Fig. 2)[29]: if $\Phi(v_1, v_2)\Psi(v_1, v_2) > 0$, then the spectral NHI at v_1 is larger than that at v_2; if $\Phi(v_1, v_2)\Psi(v_1, v_2) < 0$, then the spectral NHI at v_1 is smaller than that at v_2. The relationship was verified for spectra consisting of non-overlapping bands where the band intensities change monotonically and where the normalized intensity time dependencies do not cross (Fig. 2B).[29]

The correlation proposed by Yu et al. between the relative NHI values at v_1 and v_2 and the signs of the synchronous and asynchronous 2D-COS can be understood from Eq. (2). If the curvature of the normalized intensity time dependence at v_1 is larger than that at v_2, the NHI at v_1 will exceed that at v_2.

Multiplication of the normalized intensity spectral matrix of lower curvature at v_2 by the Hilbert–Noda matrix, followed by multiplication by the higher curvature normalized spectral intensity matrix at v_1, leads to a positive value $\Psi(v_1, v_2)$. Conversely, if the curvature of the normalized intensity time dependence at v_1 is smaller than that at v_2, the $\Psi(v_1, v_2)$ value will be negative. If the normalized intensity time dependencies at v_1 and v_2 do not cross, the intensity time dependence curvatures are directly proportional to the NHI values.

RESULTS AND DISCUSSION

2D Correlation Analysis of Simulated Spectra. Significant resolution enhancement is provided by 2D-COS. Figure 1B shows that only the overlapping B6/B7 bands can be visually resolved in the 1D simulated spectra. Figure 3 shows the 2D-COS spectra generated by correlating the simulated spectra of the non-overlapping bands B1 to B5 with the overlapping bands B6/B13. The synchronous and asynchronous spectral correlation peak features differ for the different overlapping bands due to differences in band separations, band intensities, bandwidths, and temporal intensity changes (Fig. 3).

Figure 3A shows the 2D-COS synchronous spectra. The positive signs of the autopeaks and cross-peaks in the synchronous spectrum indicate that the spectral intensity changes of all bands occur in the same direction. In this case, the 2D-COS synchronous spectrum does not provide more information than does the original 1D spectrum; no resolution improvement occurs.

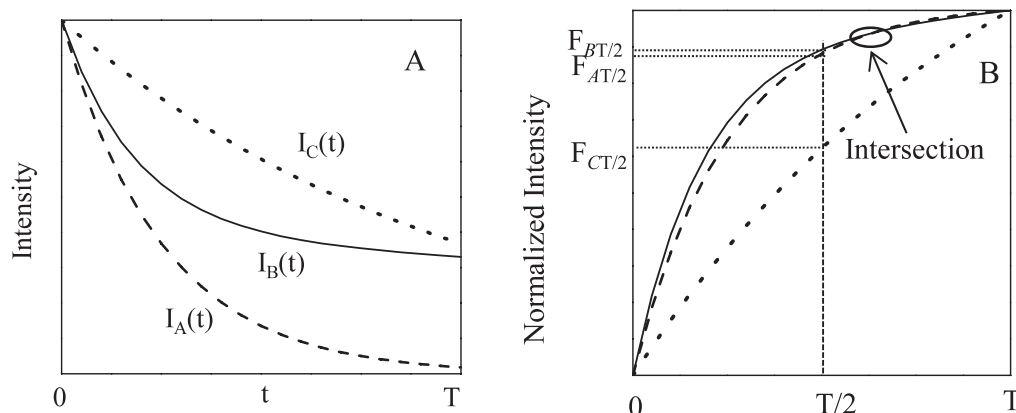The occurrence of doublet asynchronous cross-peaks with different signs in the B2, B6/B7; B3, B6/B7; B4, B6/B7; B2,

FIG. 2. (A) Time dependence of intensities of bands $I_A(t) = e^{-0.2t}$, $I_B(t) = 0.4e^{-0.01t} + 0.6e^{-0.27t}$, and $I_C(t) = e^{-0.05t}$. (B) Normalized intensity time dependence of these bands. $F_{AT/2}$, $F_{BT/2}$, and $F_{CT/2}$ refer to the NHI of these bands. The black oval shows the region where the normalized intensities of bands A and B cross.
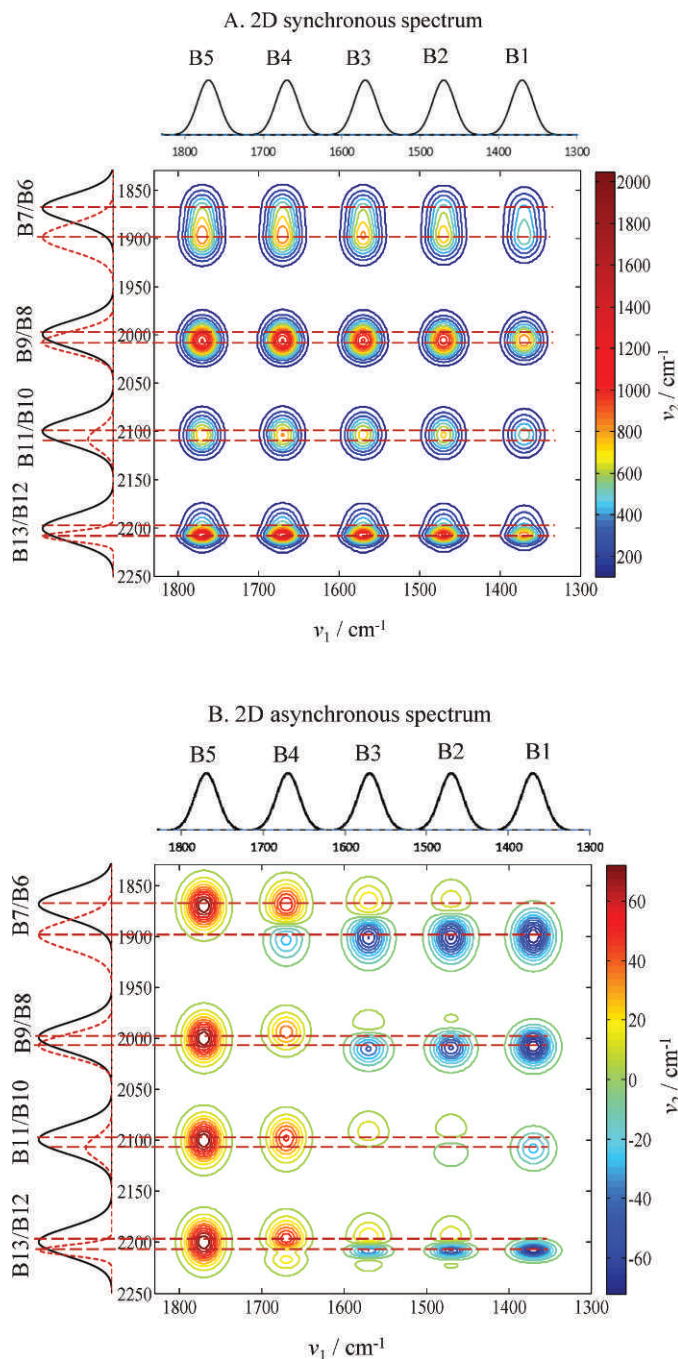
FIG. 3. **(A)** Synchronous and **(B)** asynchronous spectrum calculated from the simulated spectra of Fig. 1B. The dashed horizontal lines indicate the Gaussian band maxima.

B8/B9; B3, B8/B9; and B2, B10/B11 correlation regions in the Fig. 3B 2D asynchronous spectrum clearly resolves these overlapping bands. However, the cross-peak maxima and minima do not always correspond to the center frequencies of the overlapping Gaussian bands. This fact was previously observed and discussed.[21,24]

In the B1, B6/B7; B5, B6/B7; B1, B8/B9; B4, B8/B9; B1, B10/B11; and B3, B10/B11 correlation regions, the 2D asynchronous spectrum shows only single negative or positive cross-peaks (Fig. 3B). The low values of the correlations in

these regions indicate that the correlated bands have similar intensity change rates.

In the B5, B8/B9; B4, B10/B11; B5, B10/B11; and B5, B12/B13 asynchronous correlation regions, single cross-peaks dominate the entire overlapping-band frequency regions. The 2D-COS asynchronous spectrum does not resolve the underlying overlapping bands.

More complex triplet cross-peaks (positive, negative, and positive) are observed in the B2, B12/B13 and the B3, B12/B13 asynchronous correlation regions. Triplets of cross-peaks are expected to result from three underlying components instead of the two overlapping Gaussians here. Similar 2D-COS results were previously reported by Yu et al.[19] Further complexity is evident in the B4, B12/B13 correlation region that shows two positive cross-peaks instead of the positive and negative doublet cross-peaks commonly expected.

Modeling of the Effect of Band Overlap on Spectral Normalized Intensity. Yu et al.[29] indicates that the normalized band intensities play an important role in determining the 2D-COS spectral features. Here, we examine the mechanism of formation of 2D correlation spectra to develop deeper insight.

Given the intensities of two Gaussian bands at frequency ν and at $t = 0$, $I_{1,0}(\nu)$ and $I_{2,0}(\nu)$, an intensity matrix can be defined as:

$$I_0(\nu) = [I_{1,0}(\nu) \quad I_{2,0}(\nu)] \tag{9}$$

An intensity change coefficient matrix is defined as:

$$f = \begin{bmatrix} f1 \\ f2 \end{bmatrix} = \begin{bmatrix} f_{1,0} & f_{1,1} & f_{1,2} & \cdots & f_{1,n} \\ f_{2,0} & f_{2,1} & f_{2,2} & \cdots & f_{2,n} \end{bmatrix} \tag{10}$$

where the f1 and f2 vectors consist of component $f_{i,j}$, which are the intensity change coefficients of the ith band for the jth time or perturbation step. The spectral intensity of the overlapping bands can be calculated as:

$$I(\nu) = I_0(\nu)f = [I_{1,0}(\nu) \quad I_{2,0}(\nu)] \begin{bmatrix} f_{1,0} & f_{1,1} & f_{1,2} & \cdots & f_{1,n} \\ f_{2,0} & f_{2,1} & f_{2,2} & \cdots & f_{2,n} \end{bmatrix} \tag{11}$$

and rewritten as:

$$I(\nu) = [I_{1,0}(\nu)f_{1,0} + I_{2,0}(\nu)f_{2,0} \quad I_{1,0}(\nu)f_{1,1} + I_{2,0}(\nu)f_{2,1} \\ \cdots I_{1,0}(\nu)f_{1,n} + I_{2,0}(\nu)f_{2,n}] \tag{12}$$

For the jth perturbation time step, the normalized intensity at frequency ν:

$$F_j(\nu) = \frac{I_{1,0}(\nu)f_{1,j} + I_{2,0}(\nu)f_{2,j} - I_{1,0}(\nu)f_{1,0} - I_{2,0}(\nu)f_{2,0}}{I_{1,0}(\nu)f_{1,n} + I_{2,0}(\nu)f_{2,n} - I_{1,0}(\nu)f_{1,0} - I_{2,0}(\nu)f_{2,0}} \tag{13}$$

The normalized intensity $F_{i,j}(\nu)$ of a single Gaussian band i at the jth time step would be written as:

$$F_{i,j}(\nu) = \frac{I_{i,0}(\nu)f_{i,j} - I_{i,0}(\nu)f_{i,0}}{I_{i,0}(\nu)f_{i,n} - I_{i,0}(\nu)f_{i,0}} = \frac{f_{i,j} - f_{i,0}}{f_{i,n} - f_{i,0}} \tag{14}$$

It can be seen that $F_{i,j}(\nu)$ does not depend on frequency. Eq. (14) can be rewritten as:

$$f_{i,j} = (f_{i,n} - f_{i,0})F_{i,j} + f_{i,0} = \lambda_i F_{i,j} + \delta_i \tag{15}$$

where $\lambda_i = f_{i,n} - f_{i,0}$ and $\delta_i = f_{i,0}$. Substituting Eq. (15) into Eq. (13), the normalized intensities of overlapping bands at the jth time step can be expressed as follows:

$$F_j(\nu)$$
$$= \frac{\lambda_1 I_{1,0}(\nu)F_{1,j} + \lambda_2 I_{2,0}(\nu)F_{2,j} - \lambda_1 I_{1,0}(\nu)F_{1,0} - \lambda_2 I_{2,0}(\nu)F_{2,0}}{\lambda_1 I_{1,0}(\nu)F_{1,n} + \lambda_2 I_{2,0}(\nu)F_{2,n} - \lambda_1 I_{1,0}(\nu)F_{1,0} - \lambda_2 I_{2,0}(\nu)F_{2,0}}$$
$$(16)$$

Since $F_{1,0} = F_{2,0} = 0$ and $F_{1,n} = F_{2,n} = 1$, then $F_j(\nu)$ can be simplified:

$$F_j(\nu) = \frac{\lambda_1 I_{1,0}(\nu)F_{1,j} + \lambda_2 I_{2,0}(\nu)F_{2,j}}{\lambda_1 I_{1,0}(\nu) + \lambda_2 I_{2,0}(\nu)} \qquad (17)$$

For Gaussian bands with $I_{i,0}(\nu) = A_i e^{-\frac{(\nu - \nu_{ci})^2}{2w_i^2}}$, $F_j(\nu)$ is

$$F_j(\nu) = \frac{\lambda_1 A_1 e^{-\left[\frac{(\nu - \nu_{c1})^2}{2w_1^2}\right]}F_{1,j} + \lambda_2 A_2 e^{-\left[\frac{(\nu - \nu_{c2})^2}{2w_2^2}\right]}F_{2,j}}{\lambda_1 A_1 e^{-\left[\frac{(\nu - \nu_{c1})^2}{2w_1^2}\right]} + \lambda_2 A_2 e^{-\left[\frac{(\nu - \nu_{c2})^2}{2w_2^2}\right]}} \qquad (18)$$

The normalized spectral intensity $F_j(\nu)$ is a function of the Gaussian center frequencies (ν_{ci}), bandwidths (w_i), band amplitudes A_i, and λ_i.

Normalized Intensities of Simulated Spectra. Figure 4A shows the time and frequency dependence of the normalized simulated spectral intensities, $F_j(\nu)$. The normalized spectral intensities at the different time steps show somewhat similar profiles, except at $t = 0$ and $t = 20$ s, which are given by horizontal lines of fixed value. The NHI value of $F_{10}(\nu)$ given by $F_{T/2}(\nu) = F_{10}(\nu)$ at $t = 10$ s is shown in Fig. 4B. $F_{T/2}(\nu)$ for each of the non-overlapping B1/B5 bands have single values that are independent of frequency, except in the wings, where the adjacent band intensities begin to dominate. $F_{T/2}(\nu)$ in the overlapping band regions is frequency dependent.

Figure 4C compares the time dependence of the normalized spectral intensity $F_j(\nu)$ of the non-overlapping band B3 to the $F_j(\nu)$ of the overlapping band B12/B13 at frequencies 2162, 2202, and 2210 cm^{-1}. The normalized spectral intensities $F_j(\nu)$ monotonically increase with time. The normalized intensities $F_j(2162$ cm$^{-1})$ at all times are smaller than those of the B3 band. However, as ν increases, the $F_j(\nu)$ time dependence curve shows increasing curvature, as shown in Fig. 4C. The B3 band $F_{B_3 j}$ curve crosses that of $F_j(2202$ cm$^{-1})$ (Fig. 4C). The normalized intensity time dependence of the B3 band crosses $F_j(\nu)$ in the B12/B13 overlapping band frequency region, as well as in the other regions, which are indicated by the Fig. 4B thick, black vertical bars.

Figure 4D shows the frequency dependence of the NHI $F_{T/2}(\nu)$ in the frequency region between 1830 and 2250 cm^{-1}. In the overlapping B6/B7 frequency region, for $\nu < 1850$ cm^{-1}, $F_{T/2}(\nu)$ has the value associated with NHI of the isolated B6 band $F_{B_6 T/2}$. As the frequency increases, the B7 band begins to dominate, and $F_{T/2}(\nu)$ reaches the maximum value associated with the isolated single B7 band.

The B8/B9 and B10/B11 doublet bands overlap more than do the B6/B7 bands. Further, bands B9 and B11 are narrower than are bands B8 and B10 (Table I). The result is that bands B8 and B10 dominate only in the low-frequency wings. Thus,

the NHI of the overlapping B8/B9 and B10/B11 bands never reach the NHI values of the isolated B9 and B11 bands.

Band B13 is much narrower than is band B12, and their band center frequencies are close (Table I). In areas 3 and 4, B12 dominates, and $F_{T/2}(\nu)$ has the value of the isolated band B12, $F_{B_{12}T/2}$. Between area 3 and area 4, $F_{T/2}(\nu)$ shows a narrower peak due to the narrow B13 band contribution.

Interpretation of Asynchronous Spectral Features. Yu and coauthors discussed the relationship between the 2D-COS spectra calculated from the original spectra and from the normalized spectra:[29]

$$\Phi(\nu_1, \nu_2) = K(\nu_1)K(\nu_2)\Phi'(\nu_1, \nu_2) \qquad (19)$$

$$\Psi(\nu_1, \nu_2) = K(\nu_1)K(\nu_2)\Psi'(\nu_1, \nu_2) \qquad (20)$$

where $K(\nu_i) = I(\nu_i, T) - I(\nu_i, 0)$ is the total spectral intensity change at frequency ν_i; $\Phi'(\nu_1, \nu_2) = [1/(m-1)]\, \tilde{F}(\nu_1)^T \tilde{F}(\nu_2)$ and $\Psi'(\nu_1, \nu_2) = [1/(m-1)]\, \tilde{F}(\nu_1)^T N\tilde{F}(\nu_2)$ are the synchronous and asynchronous correlation intensities of the normalized spectra, respectively; m is the number of spectra; $\tilde{F}(\nu_i)$ is the normalized dynamic spectral intensity matrix:

$$\tilde{F}(\nu_i) = \tilde{F}(\nu_i, t) = \begin{bmatrix} \tilde{F}(\nu_i, t_1) \\ \tilde{F}(\nu_i, t_2) \\ \cdots \\ \tilde{F}(\nu_i, t_m) \end{bmatrix} \qquad (21)$$

$\tilde{F}(\nu_i, t_j)$ is the normalized dynamic spectral intensity at frequency ν_i and time t_j, defined by:

$$\tilde{F}(\nu_i, t_j) = F(\nu_i, t_j) - \frac{1}{m}\sum_{k=1}^{m} F(\nu_i, t_k) \qquad (22)$$

Normalization does not affect the relative values of the NHI.[29]

Equations (19) and (20) show that the asynchronous correlation signs and intensities depend on $K(\nu_1)K(\nu_2)$ and $\Psi'(\nu_1, \nu_2)$. If $K(\nu_1)K(\nu_2)$ is positive, the signs of $\Psi'(\nu_1, \nu_2)$ and $\Psi(\nu_1, \nu_2)$, and $\Phi(\nu_1, \nu_2)$ and $\Phi'(\nu_1, \nu_2)$ are identical. Following Yu et al.'s hypothesis,[29] given the positive values of $\Phi(\nu_1, \nu_2)$ and $\Phi'(\nu_1, \nu_2)$ (in our case), if the NHI at ν_1 is larger than that at ν_2, $\Psi'(\nu_1, \nu_2)$ and $\Psi(\nu_1, \nu_2)$ will be positive, while if the NHI at ν_1 is less than that at ν_2, $\Psi'(\nu_1, \nu_2)$ and $\Psi(\nu_1, \nu_2)$ will be negative. If the NHI of the two correlated signals are equal, then $\Psi'(\nu_1, \nu_2) = 0$. The larger the NHI difference between the two correlated bands, the larger will be $\Psi'(\nu_1, \nu_2)$.[4]

$K(\nu_1)K(\nu_2)$ is the product of the total intensity changes at frequencies ν_1 and ν_2 over the overall perturbation time range. The smaller the intensity changes, the smaller will be the $\Psi(\nu_1, \nu_2)$ correlation intensity. Thus, the correlation intensity maximum occurs at a frequency where $K(\nu_1)K(\nu_2)\Psi'(\nu_1, \nu_2)$ is a maximum. The maximum values of $K(\nu_1)K(\nu_2)$ and $\Psi'(\nu_1, \nu_2)$ occur at frequencies that are not necessarily the Gaussian center frequencies (Fig. 3D). Thus, the maximum value of $K(\nu_1)K(\nu_2)\Psi'(\nu_1, \nu_2)$ will not necessarily occur at Gaussian center frequencies (Fig. 3D).

2D Asynchronous Spectral Features Can Be Predicted from the Calculated NHI and the $K(\nu_1)K(\nu_2)$ Values. For example, in the correlation between the B3 band and the overlapping bands in the frequency regions p1, p2; p3, p4; and p7, p8, $F_{B_3 T/2}$ is smaller than $F_{T/2}(\nu)$ (Fig. 5). Thus, given Yu et al.'s hypothesis,[29] with a positive value of $K(\nu_1)K(\nu_2)$, $\Psi'(\nu_1,$
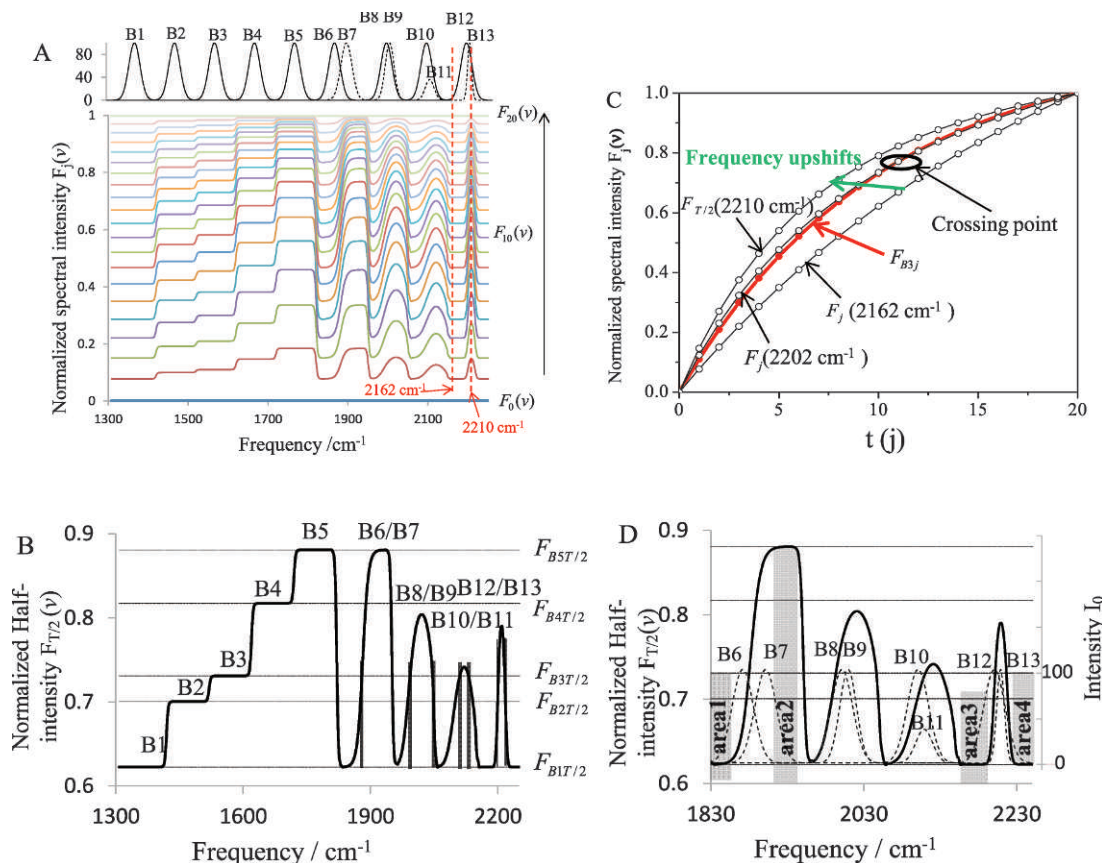
FIG. 4. (A) Frequency dependence of normalized spectral intensities $F_j(\nu)$ at different time steps. (B) NHI $F_{T/2}(\nu)$ frequency dependence of the simulated spectra. The five horizontal lines indicate the NHI of bands B1 to B5. The thick, black vertical bars indicate spectral regions where the time dependence of F_{B_3j} and $F_j(\nu)$ cross. (C) Time dependence of B3 band F_{B_3j}(1570 cm^{-1}), and of $F_j(\nu)$ at 2162, 2202, and 2210 cm^{-1}. The green arrow indicates the direction of increasing frequency, from 2162 to 2210 cm^{-1}. (D) NHI frequency dependence overlaid on the simulated Gaussian bands. The shaded bars indicate frequency regions where bands do not overlap, where single bands dominate.

ν_2) and $\Psi(\nu_1, \nu_2)$ will be negative, as observed. Asynchronous cross-peaks $\Psi(\nu_1, \nu_2)$ are expected to be positive in frequency regions where $F_{B_3T/2}$ is larger than $F_{T/2}(\nu)$ However, the $K(\nu_1)K(\nu_2)$ values in the four blue-shaded areas of Fig. 5 are very small, since the $-K(\nu_2)$ values are small. Thus, the correlation intensities $\Psi(\nu_1, \nu_2)$ between the B3 band and the overlapping bands in these areas will be very small, as observed.

The asynchronous correlation peak intensities $\Psi(\nu_1, \nu_2)$ also depend on the relative values of $F_{T/2}(\nu)$ of the overlapping bands and $F_{B_3T/2}$. In the frequency region p5, p6, $F_{B_3T/2}$ is slightly smaller than $F_{T/2}(\nu)$. Thus, the 2D correlation will give vanishingly small cross-peaks. All of these conclusions are verified in the calculated 2D asynchronous spectrum.

At frequencies around points p1–p8 (Fig. 5), the time dependencies of the normalized intensities cross that of band B3 (black vertical bars in Fig. 4B). This crossing makes the signs of $\Psi(\nu_1, \nu_2)$ not predictable from Yu et al.'s conclusions. As shown in Fig. 4C, the time dependence $F_j(\nu)$ curvature increases as the frequency increases. Thus, the normalized intensity difference between the B3 band and the overlapping bands between 2162 and 2210 cm^{-1} decrease monotonically $[F_{B_3T/2}-F_{T/2}(\nu)]$ as the frequency increases. Thus, the 2D asynchronous correlation intensities $\Psi(\nu_1, \nu_2)$ decrease monotonically, from positive to negative in the frequency range between 2162 to 2210 cm^{-1}. At frequencies close to p7 = 2202

cm^{-1}, the 2D correlation asynchronous intensities will be very small. Similar situations will occur whenever the normalized intensities of correlated bands cross.

Interpretation of the B3, B12/B13 Correlation Spectral Feature. In the B12/B13 band frequency region, the overlapping B13 band is much narrower than is the B12 band. The separation between these bands is small (Fig. 4D). The overlapping B12/B13 band $F_{T/2}(\nu)$ peak has a much narrower bandwidth than does the difference spectrum between the simulated spectral at $t = 0$ and $t = 20$ s, $-K(\nu_2)$ (Fig. 5).

Between points O$_1$ and p7 (Fig. 5), $F_{B3T/2}$ is larger than that of the B12/B13 band $F_{T/2}(\nu)$. Thus, the asynchronous cross-peak $\Psi(\nu_1, \nu_2)$ will be positive. In contrast, in the frequency region between p7 and p8, $F_{B3T/2}$ is smaller than $F_{T/2}(\nu)$, forcing the asynchronous cross-peak $\Psi(\nu_1, \nu_2)$ to be negative. In the frequency region between p8 and O$_2$, $F_{B3T/2}$ is again larger than $F_{T/2}(\nu)$. The values of $K_1(\nu_1)K_2(\nu_2)$ are sufficiently large enough to generate a positive cross-peak. Thus, triplet asynchronous cross-peaks are generated in the B3, B12/B13 correlation region.

Interpretation of the B4, B12/B13 Correlation Spectral Feature. Figure 5 shows that in the overlapping B12/B13 band region, $F_{B_4T/2}$ is always larger than $F_{T/2}(\nu)$. Thus, positive asynchronous cross-peaks will occur. However, since the difference between $F_{B_4T/2}$ and $F_{T/2}$(2210 cm^{-1}) is small, $\Psi'(\nu_1, \nu_2)$ will be small. Thus, the asynchronous correlation intensity
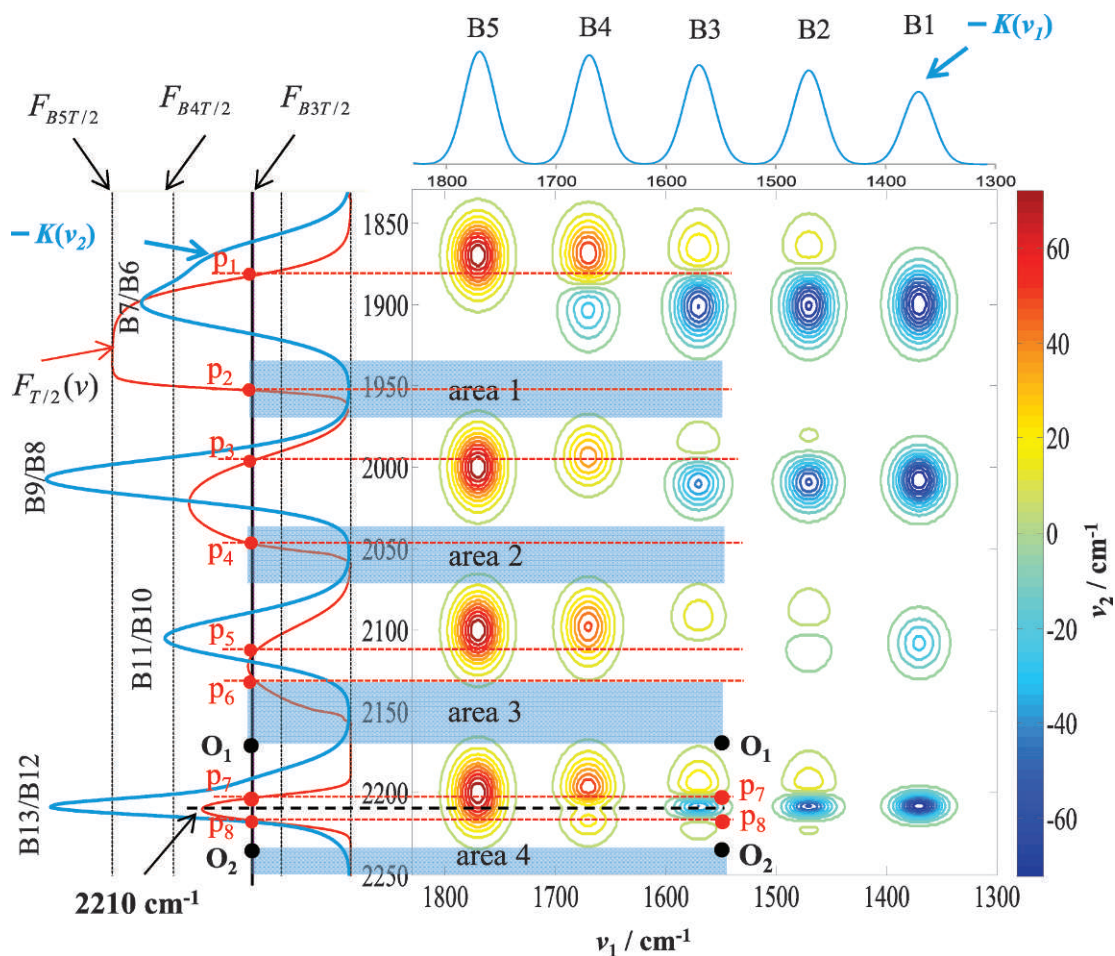
FIG. 5. Asynchronous 2D correlation spectrum and the NHI frequency dependence, $F_{T/2}(\nu)$. $F_{T/2}(\nu)$ along left vertical axis (red curve) overlaid with the difference spectrum between the simulated spectra at $t = 0$ and $t = 20$ s $[-K(\nu_2) = I(\nu_2,0) - I(\nu_2, 20)]$ (blue line) in the overlapping band regions. The four horizontal, blue-shaded areas indicate regions of small $-K(\nu_2)$ values. O_1 and O_2 label the edges of areas 3 and 4. The black vertical line indicates the value of the NHI of the B3 band. Points p1 to p8, along the black vertical line, indicate frequencies where $F_{B_3T/2} \approx F_{T/2}(\nu)$. p1 = 1882 cm^{-1}, p2 = 1952 cm^{-1}, p3 = 1994 cm^{-1}, p4 = 2046 cm^{-1}, p5 = 2112 cm^{-1}, p6 = 2128 cm^{-1}, p7 = 2202 cm^{-1}, p8 = 2216 cm^{-1}. The top horizontal spectrum shows the B1–B5 band difference spectrum between $t = 0$ and $t = 20$ s $[-K(\nu_2) = I(\nu_2,0) - I(\nu_2, 20)]$.

$K_1K_2\Psi'(\nu_1, \nu_2)$ at 2210 cm^{-1} will be weak. The correlation of band B4 with the overlapping B12/B13 bands generates two positive asynchronous cross-peaks, with a minimum between them at 2210 cm^{-1}.

Overlapping Band Resolution. It can be seen in Fig. 5 that all of the overlapping bands are clearly resolved in correlations with the B2 and B3 bands. In contrast, the correlation with band B5 does not give clear resolution. Good resolution requires that the NHI of a single correlating band have a value between the maximum and minimum of the NHI of the overlapping correlating bands. These observations suggest a useful 2D-COS method to analyze highly overlapping bands. Spectral resolution would be enhanced by correlating complex spectra with simulated single-band spectra with variable intensity change rates.

2D Correlation Analysis of Spectra Simulated by Using Lorentzian Function. We performed a similar study by using Lorentzian functions with the same band parameters. While the contour shape of 2DCOS spectral peaks change because of the differing Lorentzian band shape, most of the Gaussian band 2D-COS features remain. The Lorentzian 2D-COS spectral features can be explained identically as for the Gaussian band shapes by using the total intensity changes and normalized half-intensities.

CONCLUSION

Our study shows that spectral normalized intensities are important in determining the 2D-COS spectral intensities. The signs and number of 2D cross-peaks are related to the NHI differences and the total intensity changes of the correlated bands. These insights into the origin of the 2D spectral features will help interpret the 2D asynchronous COS spectra. Our results indicate a good method to help resolve overlapping bands. This method would correlate the overlapping band regions with a series of discrete bands of different intensity change rates.

1. I. Noda. "Two-Dimensional Infrared (2D IR) Spectroscopy of Synthetic and Biopolymer". Bull. Am. Phys. Soc. 1986. 31:520.

2. I. Noda. "Two-Dimensional Infrared Spectroscopy". J. Am. Chem. Soc. 1989. 111(21): 8116-8118.

3. I. Noda. "Generalized Two-Dimensional Correlation Method Applicable to Infrared, Raman, and Other Types of Spectroscopy". Appl. Spectrosc. 1993. 47(9): 1329-1336.

4. I. Noda, Y. Ozaki. Two-Dimensional Correlation Spectroscopy: Applications in Vibrational and Optical Spectroscopy. Chichester, UK: John Wiley and Sons, Ltd., 2004.

5. L. Ashton, B. Czarnik-Matusewicz, E.W. Blanch. "Application of Two-Dimensional Correlation Analysis to Raman Optical Activity". J. Mol. Struct. 2006. 799(1-3): 61-71.

6. M.A. Czarnecki, B. Czarnik-Matusewicz, Y. Ozaki, M. Iwahashi. "Resolution Enhancement and Band Assignments for the First Overtone of OH(D) Stretching Modes of Butanols by Two-Dimensional Near-Infrared Correlation Spectroscopy. 3. Thermal Dynamics of Hydrogen Bonding in Butan-1-(ol-D) and 2-Methylpropan-2-(ol-D) in the Pure Liquid States". J. Phys. Chem. A. 2000. 104(21): 4906-4911.

7. V.A. Shashilov, I.K. Lednev. "2D Correlation Deep UV Resonance Raman Spectroscopy of Early Events of Lysozyme Fibrillation: Kinetic Mechanism and Potential Interpretation Pitfalls". J. Am. Chem. Soc. 2008. 130(1): 309-317.

8. V.A. Shashilov, I.K. Lednev. "Two-Dimensional Correlation Raman Spectroscopy for Characterizing Protein Structure and Dynamics". J. Raman Spectrosc. 2009. 40(12): 1749-1758.

9. I. Noda. "Progress in 2D Correlation Spectroscopy". AIP Conf. Proc. 2000. 503: 3-17.

10. M.A. Czarnecki, H. Maeda, Y. Ozaki, M. Suzuki, M. Iwahashi. "Resolution Enhancement and Band Assignments for the First Overtone of OH Stretching Modes of Butanols by Two-Dimensional Near-Infrared Correlation Spectroscopy. 2. Thermal Dynamics of Hydrogen Bonding in n-and tert-Butyl Alcohol in the Pure Liquid States". J. Phys. Chem. A. 1998. 102(46): 9117-9123.

11. M.A. Czarnecki, H. Maeda, Y. Ozaki, M. Suzuki, M. Iwahashi. "Resolution Enhancement and Band Assignments for the First Overtone of OH Stretching Mode of Butanols by Two-Dimensional Near-Infrared Correlation Spectroscopy. Part I: sec-Butanol". Appl. Spectrosc. 1998. 52(7): 994-1000.

12. Y. Ozaki, I. Noda. "Potential of Generalized Two-Dimensional Correlation Spectroscopy in the Near Infrared Region". J. Near Infrared Spec. 1996. 4(1-4): 85-99.

13. I. Noda. "Progress in Two-Dimensional (2D) Correlation Spectroscopy". J. Mol. Struct. 2006. 799(1–3): 2-15.

14. I. Noda. "Two-Dimensional Correlation Spectroscopy—Biannual Survey, 2007–2009". J. Mol. Struct. 2010. 974(1-3): 3-24.

15. I. Noda. "Two-Dimensional Infrared (2D IR) Spectroscopy: Theory and Applications". Appl. Spectrosc. 1990. 44(4): 550-61.

16. B. Hinterstoisser, L. Salmen. "Two-Dimensional Step-Scan FTIR: a Tool to Unravel the OH Valency Range of the Spectrum of Cellulose I". Cellulose. 1999. 6(3): 251-263.

17. A. Filosa, Y. Wang, A.A. Ismail, A.M. English. "Two-Dimensional Infrared Correlation Spectroscopy as a Probe of Sequential Events in the Thermal Unfolding of Cytochrome c". Biochemistry. 2001. 40(28): 8256-8263.

18. H. Huang, Z. Ye, J. Chen, H. Chen. "Concerning the Spectral Resolution Enhancement of Dynamic 2D-IR". Vib. Spectrosc. 2009. 49(2): 251-257.

19. Z. Yu, Y. Wang, J. Liu. "Overlap May Cause Misleading Results in Two-Dimensional Correlation Spectra". Appl. Spectrosc. 2005. 59(3): 388-391.

20. M.A. Czarnecki. "Interpretation of Two-Dimensional Correlation Spectra: Science or Art?". Appl. Spectrosc. 1998. 52(12): 1583-1590.

21. M.A. Czarnecki. "Two-Dimensional Correlation Spectroscopy: Effect of Band Position, Width, and Intensity Changes on Correlation Intensities". Appl. Spectrosc. 2000. 54(7): 986-993.

22. T. Lefevre, K. Arseneault, M. Pezolet. "Study of Protein Aggregation Using Two-Dimensional Correlation Infrared Spectroscopy and Spectral Simulations". Biopolymers. 2004. 73(6): 705-715.

23. S.-I. Morita, Y. Ozaki. "Pattern Recognitions of Band Shifting, Overlapping, and Broadening Using Global-Phase Description Derived from Generalized Two-Dimensional Correlation Spectroscopy". Appl. Spectrosc. 2002. 56(4): 502-508.

24. A. Gericke, S.J. Gadaleta, J.W. Brauner, R. Mendelsohn. "Characterization of Biological Samples by Two-Dimensional Infrared Spectroscopy: Simulation of Frequency, Bandwidth, and Intensity Changes". Biospectroscopy. 1996. 2(6): 341-351.

25. M.A. Czarnecki. "Two-Dimensional Correlation Analysis of Hydrogen-Bonded Systems: Basic Molecules". Appl. Spectrosc. Rev. 2011. 46(1): 67-103.

26. S.R. Ryu, I. Noda, C.H. Lee, P.H. Lee, H. Hwang, Y.M. Jung. "Two-Dimensional Correlation Analysis and Waterfall Plots for Detecting Positional Fluctuations of Spectral Changes". Appl. Spectrosc. 2011. 65(4): 359-368.

27. M.A. Czarnecki. "Frequency Shift or Intensity Shift? The Origin of Spectral Changes in Vibrational Spectra". Vib. Spectrosc. 2012. 58: 193-198.

28. I. Noda. "Determination of Two-Dimensional Correlation Spectra Using the Hilbert Transform". Appl. Spectrosc. 2000. 54(7): 994-999.

29. Q. Jia, N.-N. Wang, Z.-W. Yu. "An Insight into Sequential Order in Two-Dimensional Correlation Spectroscopy". Appl. Spectrosc. 2009. 63(3): 344-353.

APPENDIX A: LIST OF SYMBOLS

A_i	Maximum amplitude of the ith Gaussian band
f	An intensity change coefficient matrix
f_i	Intensity change coefficient of the band B_i
$f_{i,j}$	Intensity change coefficient of the ith band for the jth time step
$F_{i,j}(\nu)$	Normalized intensity of a single Gaussian band i at the jth time step
$F_j(\nu)$	Normalized intensity at jth time step at frequency ν
$\tilde{F}(\nu_i)$	Normalized dynamic spectral matrix
$F_{B_i T/2}$	Normalized half-intensity of B_i band
$F_{T/2}(\nu)$	Normalized half-intensity at frequency ν
$I_0(\nu)$	Intensities matrix of simulated Gaussian bands at frequency ν
$I_{i,0}(\nu)$	Intensities of simulated Gaussian band i at frequency ν
$I(\nu, t)$	Intensity of simulated spectra at frequency ν and at time t
k_i	Intensity change rate constant of band B_i
K_i	Total intensity change of spectra during the perturbation at ν_i
m	Number of spectra collected over perturbation
w_i	Full band width at half height $= 2(2\ln 2)^{1/2} w_i$
$y(\nu_i, t_j)$	Measured spectral signal at ν_i and time t_j
$\tilde{y}(\nu_i)$	Dynamic spectral intensity matrix
$\tilde{y}(\nu_i, t_j)$	Dynamic spectral signal at ν_i and time t_j
λ_i	Total change of intensity change coefficient of band B_i during the perturbation period
ν	Frequency
ν_{ci}	Gaussian center frequency
$\Phi(\nu_1, \nu_2)$	Synchronous correlation intensity
$\Phi'(\nu_1, \nu_2)$	Synchronous correlation intensity of normalized spectra
$\Psi(\nu_1, \nu_2)$	Asynchronous correlation intensity
$\Psi'(\nu_1, \nu_2)$	Asynchronous correlation intensity of normalized spectra